Study of opposite-sign dimuon production in high-energy neutrino-nucleon interactions

B. Strongin,* J. Bofill,† J. I. Friedman, S. Fuess,† M. C. Goodman,‡ H. W. Kendall,
V. Kistiakowsky, T. Lyons,† L. S. Osborne, R. Pitt,§ U. Schneekloth,** and F. E. Taylor
Massachusetts Institute of Technology, Cambridge, Massachusetts 02139

D. Bogert, G. Koizumi, and L. Stutte
Fermi National Accelerator Laboratory, Batavia, Illinois 60510

M. Abolins, R. Brock, W. Cobau, R. Hatcher, D. Owen, G. Perkins,
M. Tartaglia,† and H. Weerts
Michigan State University, E. Lansing, Michigan 48824

R. Belusevic,†† J. K. Walker, A. White, and J. Womersley‡‡
University of Florida, Gainsville, Florida 32611
(Received 1 October 1990)

Results are presented of a study of opposite-sign dimuon events observed in a fine-grained neutrino detector exposed to the Fermilab Tevatron wide-band neutrino beam. A total of 300 background-corrected $\mu^+\mu^-$ events induced by incident neutrinos and antineutrinos with energies up to 500 GeV were accumulated. The data were analyzed in terms of a model based on charm-quark production followed by semileptonic decay of the charmed meson. The Cabibbo-Kobayashi-Maskawa matrix terms were found to be $|U_{cd}|^2 = 0.0378 \pm 0.0127$ (stat)$^{+0.0099}_{-0.0082}$ (syst), and $\kappa|U_{cs}|^2 = 0.391 \pm 0.076$ (stat)$^{+0.097}_{-0.066}$ (syst). The ratio of the strange to nonstrange sea in the nucleon, $\kappa = 2S/(\overline{U} + \overline{D})$, was measured to be 0.407 ± 0.075 (stat)$^{+0.103}_{-0.069}$ (syst).

I. INTRODUCTION

An attractive feature of opposite-sign dimuon production in neutrino-nucleon scattering is that it provides a window to the sea of nonvalence quarks in the nucleon. In particular, the data allow the abundance of strange quarks relative to nonstrange quarks to be determined. According to our present understanding, this abundance is controlled by Q^2-dependent QCD effects. Another benefit of a measurement of dimuons is that it permits a determination of the charged-current coupling strength of the charm quark with the down and the strange quarks. Given the new high-energy region opened up by the Fermilab Tevatron wideband neutrino beam, it was worthwhile to reexamine this process in a new high-energy region where there was the possibility that some new phenomenon may be uncovered.

The data of this study were obtained using a 340 metric ton fine-grained calorimeter[1] exposed to the quadrupole triplet wideband neutrino beam (QTB) at Fermilab. The pattern-recognition capabilities of the detector were useful in extracting the small dimuon signal and in studying its kinematic properties. The QTB offered a unique opportunity to study opposite-sign dimuon production at the highest available accelerator energies. Events were recorded with neutrino energies up to about 500 GeV.

After a brief discussion in Sec. II of the standard model of opposite-sign dimuon production, the details of the apparatus, event selection, background correction, incident-neutrino-flux normalization, and Monte Carlo

simulation are described in Sec. III. The results are given in Sec. IV. There, several fits of the data to the standard model are discussed and the systematic errors of the fits are estimated. A summary is given in Sec. V.

II. THEORY

In the standard model, opposite-sign dimuons are produced in neutrino-nucleon scattering through the charged-current interaction where a charm (c) quark is created from a down (d) or a strange (s) quark. The c quark forms a charmed particle (most frequently a D meson) which may decay semileptonically into a muon with a charge opposite that of the outgoing muon from the primary neutrino-nucleon vertex. The process is depicted schematically in Fig. 1.

The cross section for opposite-sign dimuon production for incident neutrinos for an isoscalar target is given by[2]

$$d^3\sigma^\nu/dx\,dy\,dz = (G_F^2 ME_\nu/2\pi)\xi\{[u(\xi)+d(\xi)]|U_{cd}|^2$$

$$+2s(\xi)|U_{cs}|^2\}$$

$$\times(1-m_c^2/2ME_\nu\xi)D(z)B_c \ , \qquad (1)$$

where G_F is the Fermi constant; E_ν is the incident neutrino energy; M is the nucleon mass; U_{cd} and U_{cs} are Cabibbo-Kobayashi-Maskawa (CKM) matrix elements;[3] $u(\xi)$, $d(\xi)$, and $s(\xi)$ are the up-, down-, and strange-quark structure functions, respectively. The large effective mass of the charm quark m_c expected to be of
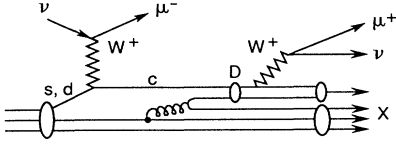
FIG. 1. The diagram depicting the production of opposite-sign dimuon events in high-energy deep-inelastic neutrino-nucleon scattering. The initial neutrino interacts with the nucleon by means of W^+ exchange with a down or strange quark to produce a charm quark, which fragments into a D meson, subsequently decaying semileptonically into a positive muon.

order 1.5 GeV/c^2 gives rise to an energy threshold that is taken into account by replacing the usual scaling variable $x = Q^2/2ME_\nu y$ by the slow-rescaling variable[4] $\xi = x + m_c^2/2ME_\nu y$, and by multiplying the cross section by the helicity factor $(1 - m_c^2/2ME_\nu \xi)$. $D(z)$ is the fragmentation function of the charm quark to form a charmed meson of momentum fraction z relative to the c quark. B_c is the inclusive branching ratio for muonic decays of the charmed meson. The corresponding cross section for incident antineutrinos is obtained by replacing the quark with antiquark distributions in Eq. (1). For neutrino-induced events the contributions from d and s quarks are roughly equal, whereas for incident antineutrinos essentially all dimuon events are produced from the "Cabibbo-favored" $\bar{s}$-to-$\bar{c}$-quark charged-current transition.

Analyzing the opposite-sign dimuon data in terms of the model described above allows several important physical parameters to be determined. The effective mass of the charm quark m_c can be measured by studying the threshold behavior of the dimuon rate normalized to the single-muon rate as a function of the incident neutrino energy. Not only is this of interest in its own right as a probe of a nonperturbative QCD effect, but also a precise knowledge of the m_c parameter is important in high-precision measurements of $\sin^2\theta_W$ in deep-inelastic neutrino-nucleon scattering.[5] The terms $|U_{cd}|^2$ and $\kappa|U_{cs}|^2$, where $\kappa = 2S/(\bar{U} + \bar{D})$ is the ratio of the strange to nonstrange sea, can be determined by fitting the distribution of the Bjorken x variable computed from experimentally accessible quantities, $x_{vis} = Q_{vis}^2/2M\nu_{vis}$, to the cross-section form given in Eq. (1). The terms S, $\bar{U}$, and $\bar{D}$ are the integrals of the strange, up, and down sea-quark distributions, respectively, where for example $S = \int \xi s(\xi, \hat{Q}^2)d\xi$ and $\hat{Q}^2$ is the mean Q^2 of the data. In the evaluation of x_{vis} we define $\nu_{vis} = E_{shower} + E_{\mu2}$ and $Q_{vis}^2 = 4(\nu_{vis} + E_{\mu1})E_{\mu1}\sin^2(\theta_{\mu1}/2)$, where E_{shower} is the energy of the hadronic shower, $E_{\mu1,2}$ are the muon energies ($E_{\mu1} > E_{\mu2}$ by definition), and $\theta_{\mu1}$ is the angle of the leading muon with respect to the incident neutrino direction. Further separation of the CKM term $|U_{cs}|$ and κ can be effected if assumptions about either the unitarity or the form of the CKM matrix are made. The branching ratio B_c and the quark fragmentation function $D(z)$ also enter the model and thus in principle can be deter-

mined from the dimuon data. The correlations of these terms with each other and with the CKM terms are strong however, and to proceed it is expedient to assume a value of B_c and a form of $D(z)$ derived from independent sources, such as neutrino emulsion[6] and e^+e^- experiments.[7]

III. EXPERIMENTAL DETAILS

In this section we describe the apparatus, event selection, background correction, neutrino flux, and Monte Carlo simulation of the experiment.

A. Apparatus

We discuss here only those features of the apparatus that were unique to this measurement since the detector has been described in detail elsewhere.[8] The neutrino detector, located in Lab C at Fermilab, was constructed from plastic flash chambers, which provided a fine-grained sampling of the energy deposition of the event, and aluminum proportional tube chambers, which were
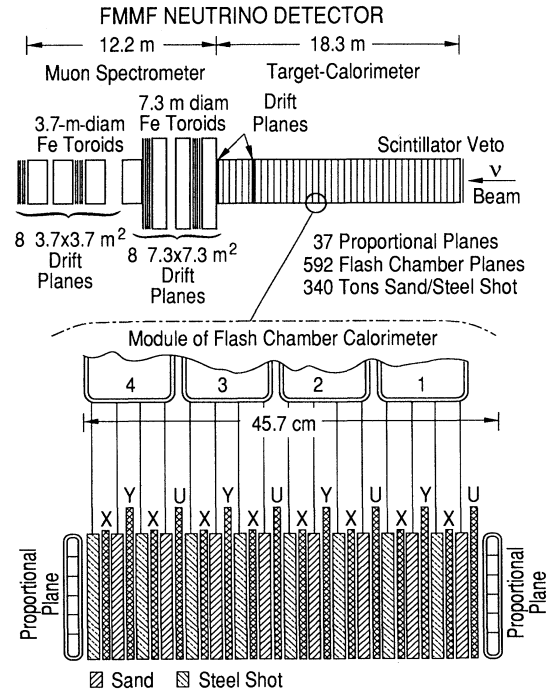
FIG. 2. General layout of the flash-chamber–proportional-tube calorimeter and details of a module. The active part of the calorimeter was about 18.3 m long and had a cross-sectional area of about 3.65×3.65 m². The flash chamber planes alternated in an U-X-Y-X pattern, where X chambers had their cells running horizontally, U and Y chambers had their cells ±10° about the vertical direction. The proportional tube chambers were placed every 16 flash chambers with their wires in a horizontal-vertical alternating pattern. The material of the calorimeter was sand (SiO_2) and steel shot (Fe) contained in plastic extrusions. Drift-chamber planes were located in two positions at the rear of the calorimeter and in the iron toroidal spectrometer as indicated.

used to trigger the calorimeter and to provide another measure of deposited energy.[9] A veto counter was placed in front of the detector to avoid triggering on upstream neutrino interactions. Behind the 18.3-m-long calorimeter was a set of solid iron toroidal magnets (three 7.3-m diameter and four 3.7-m diameter). These were instrumented with drift chambers to allow muons to be identified and their momenta to be measured. Drift chambers were also placed in two locations at the rear of the calorimeter to provide accurate entry points and angles of muons entering the toroid spectrometer. The 7.3-m-diameter toroids were important for good acceptance of large-angle, high-Q^2 muons. Figure 2 is a schematic view of the main components of the detector.

B. Event selection

During a run of the QTB at Fermilab we employed a mixture of hardware triggers to enhance the fraction of dimuon events (< 1%) and other rare processes as well as record charged-current deep-inelastic scattering events. Dimuon events were selected by software as those with two identified penetrating tracks emerging from the primary neutrino-nucleon interaction vertex. To ensure a clean event sample, fiducial volume constraints, hit requirements in the toroid spectrometer, and hadron and muon energy cuts were imposed. The fiducial volume cuts required the event vertex to be between chambers 41 and 400 (out of a total of 592) along the beam direction. For lateral confinement, the vertex was required to be within 100 cm of the beam axis. These cuts ensured that at least 7.5 interaction lengths longitudinally and one interaction length laterally were available to contain the hadron shower. The hadron energy was required to satisfy $E_h > 10$ GeV, to ensure that the efficiency of all electronic triggers contributing to the dimuon sample was 100%. The muon-energy cuts, specified by $E_{\mu 1,2} > 10$ GeV, were chosen on the basis of event-reconstruction efficiency and background rejection.

Monte Carlo simulations of both single-muon and dimuon events were performed. These simulations included the details of the hadronic shower development,[10] noise hits in the flash chamber calorimeter and drift system, and the experimental details of the muon track reconstruction. The Monte Carlo "events" were subsequently analyzed by the same event-reconstruction software as was used for the data.

We designed our analysis of the dimuon data in such a way as to reduce our sensitivity to the details of the Monte Carlo simulation. By treating the dimuon data as a *ratio* to single-muon data, only the *relative* reconstruction efficiencies were important. From the Monte Carlo studies we found that the single-muon event-reconstruction efficiency for neutrino-induced events satisfying the cuts defined above was (95±0.34)% and the dimuon reconstruction efficiency was (90±0.46)%.

The event selection algorithms were further checked against a dimuon data sample culled from unbiased triggers by a visual scan. Finally each computer-selected event was scanned independently by physicists to eliminate "pathological" events. The data sample consisted of 393 opposite-sign dimuon events after acceptance cuts but before the background correction, and 68 000 single-muon charged-current events. (Note that these two event
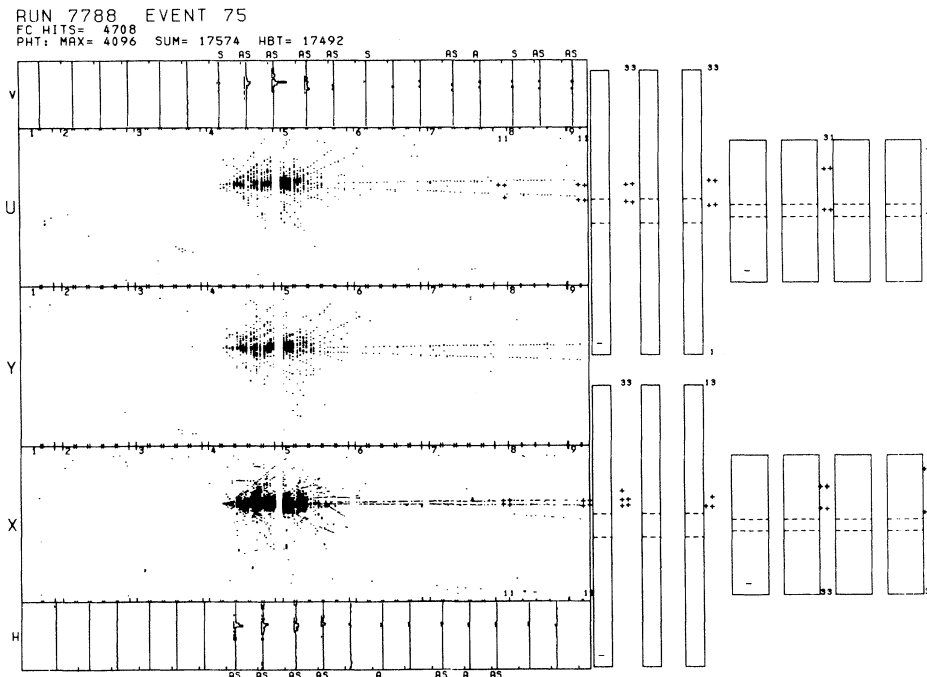
FIG. 3. A typical dimuon event in the detector. Each dot in the flash chamber calorimeter display of the hadronic shower and muon tracks denotes a 5×5-mm^2 cell. The bending of the muons in the toroidal magnetic field is evident.

types were taken with different trigger prescaling factors precluding a simple comparison as a measure of the relative dimuon rate.) Figure 3 shows a typical dimuon event.

C. Background correction

The dominant source of background in our dimuon data sample arose from decays of hadrons produced either in the primary neutrino-nucleon interaction or in the subsequent hadronic shower. The flux of decay muons from the first source was computed from the multiplicities and momentum distributions of the primary pions and kaons given by a Lund Monte Carlo[11] simulation of deep-inelastic charged-current neutrino-nucleon scattering. The muons from the second source were estimated by summing the muon yields of each component of the hadronic shower initiated by each nondecaying primary hadron given by the Lund Monte Carlo program. These separate yields were determined from a parametrization of the measured muon fluxes emanating from hadron showers of calibration data taken with a hadron beam of various energies incident on the calorimeter.[12]

The reconstruction efficiency and acceptance of the decay background were simulated by using like-sign dimuon events. This class of events has been shown to be dominated by nonprompt decays of hadrons (mostly pions and kaons) in charged-current events.[13] With our low-density calorimeter ($\rho = 1.38$ g/cm^3) we expected that the hadron decay contribution to like-sign dimuons would be even larger than those of Ref. 13. We identified 57 $\mu^-\mu^-$ and 8 $\mu^+\mu^+$ events which we found to be consistent with this decay background. The measured and calculated (from hadron decay) like-sign dimuon rates for the acceptance cuts given above, normalized to single-muon events that have been corrected for the trigger prescaling factor, are given in Table I.

To estimate the background for the opposite-sign dimuon signal, the like-sign data were scaled by the Monte Carlo–calculated ratio of opposite-sign to like-sign decay rate as a function of hadron energy. Use of this technique made the background estimate relatively insensitive to the details of the simulation. Other background sources such as trimuon production were considered and found to be negligible.[14] From these studies we concluded that 93±15 (statistical and systematic errors combined) opposite-sign dimuon events, or 24% of the raw data sample, were attributable to background sources. Thus, the dimuon signal consisted of 300±25 events, where the error includes the statistical uncertain-

TABLE II. The number of dimuon events of various categories. Shown are the observed, and the corrected number of events in each sign combination. The like-sign events, corrected by the Monte Carlo calculation to estimate the number of opposite-sign events from decay, are given in the "corrected" rows.

Event type	Number of events
$\mu^-\mu^+$	393
$\mu^-\mu^-$	57
$\mu^+\mu^+$	8
Corrected $\mu^-\mu^-$	79
Corrected $\mu^+\mu^+$	14
$\mu^-\mu^+$ after background subtraction	300

ty of the data and systematic error of the background subtraction. Each experimental distribution was corrected by this method for the decay background bin by bin. Table II summarizes the number of dimuon events in our data sample.

D. Neutrino flux

The neutrino beam was produced by allowing 800-GeV protons to interact with a beryllium oxide powder target thereby producing pions and kaons, a fraction of which were focused (point to parallel at 300 GeV/c) by a set of quadrupole magnets.[15] These pions and kaons were then allowed to decay in an evacuated pipe to produce neutrinos and antineutrinos. Muons and hadrons remaining in the secondary beam were absorbed by iron and earth shielding placed before the detector.

There was no sign selection of secondary pions and kaons, and thus the QTB consisted of both neutrinos and antineutrinos. We determined the antineutrino-neutrino composition of the beam by using the number of observed deep-inelastic charged-current events, classified according to the sign of the outgoing muon, and a Monte Carlo simulation. The result was the ratio of antineutrino-to-neutrino fluxes integrated over the energy range of the data: $\Phi_{\bar{\nu}}/\Phi_\nu = (N_{\mu+}\hat{\sigma}_\nu/N_{\mu-}\hat{\sigma}_{\bar{\nu}}) = 0.342 \pm 0.007$ (stat) ± 0.014 (syst), where $\Phi_\nu = \int_{E_{\text{total}}}(d\Phi_\nu/dE_\nu)dE_\nu$, $N_{\mu-}$ is the number of observed neutrino events above an energy cut $E_{\text{total}} = 20$ GeV, and $\hat{\sigma}_\nu$ is the neutrino-nucleon scattering cross section averaged over the incident neutrino flux,[16] with antineutrino quantities $\Phi_{\bar{\nu}}$, $N_{\mu+}$, and $\hat{\sigma}_{\bar{\nu}}$ defined in a similar manner. A small correction ($\langle 0.8\% \rangle$) was applied to compensate for outgoing muons with signs that were misclassified by the software. The systematic error reflects the dispersion of the various measurements of the total neutrino and antineutrino cross-section ratio $\sigma_\nu/\sigma_{\bar{\nu}}$.[17]

E. Monte Carlo simulations

The Monte Carlo simulations of the dimuon and single-muon data took into account the details of the incident neutrino beam, the detector acceptances, resolu-

TABLE I. A comparison of the measured and calculated like-sign dimuon rates normalized to the single-muon data. The agreement between these numbers indicates that the like-sign data in this experiment arose mostly from decay of hadrons in the recoil hadronic shower.

	$\mu^-\mu^-$ rate	$\mu^+\mu^+$ rate
Measured:	$(6.52\pm0.86)\times10^{-4}$	$(5.76\pm2.03)\times10^{-4}$
Calculated	$(5.91\pm0.14)\times10^{-4}$	$(4.01\pm0.12)\times10^{-4}$

tion smearing, efficiency of event selection software, and the details of the physics of both processes. The valence and nonstrange sea-quark structure functions were computed according to the prescription of Ref. 16. The strange-quark structure functions were taken to have the same shape as the nonstrange sea distribution, but with a magnitude which was allowed to vary by the parameter κ. It was assumed that $\xi \bar{u}(\xi, Q^2) = \xi \bar{d}(\xi, Q^2)$ and $\xi \bar{s}(\xi, Q^2) = \xi s(\xi, Q^2)$. The dimuon data were at a mean observed $\langle Q^2_{\text{vis}} \rangle \approx 25$ (GeV/c)^2 which, on the basis of the simulation of opposite-sign dimuon production, corresponded to $\langle Q^2 \rangle \approx 28$ (GeV/c)^2.

The emulsion data of Ushida *et al.*[6] were used to determine the ratio of charmed-meson (D and D^*) to charmed-baryon production in our neutrino beam. These data indicated that the source of the second muon was primarily D-meson decays at high energies. To fix the inclusive branching ratio of D mesons to muons, SLAC Mark III e^+e^- data[7] were used, weighted by the D^0/D^+ production ratio according to the analysis of Gilman, Kleinknecht, and Renk.[6] The matrix element for three-body semileptonic decay was taken from Ref. 18. The transverse-momentum distribution of the decay muon relative to the parent charm quark was parametrized by $dN/dp_t^2 \propto \exp(-1.1p_t^2)$,[19] where p_t is in GeV/c.[19] The formation of the charmed meson was simulated by the Peterson fragmentation function $D(z)$ with the shape parameter $\epsilon = 0.19 \pm 0.03$.[20]

The Monte Carlo simulations of the beam and nucleon structure functions were checked by comparing them with single-muon data. A small empirical correction had to be applied to the reconstruction efficiency for low-momentum muons ($p_\mu < 20$ GeV/c) to achieve better agreement with the data. This same correction was applied to the dimuon data.

IV. RESULTS

Based on the estimated dimuon cross sections and the incident neutrino and antineutrino fluxes, the antineutrino production of dimuons in our data sample was expected to be only about 20% of the neutrino production. Since this was a small fraction of the total event sample, and to avoid introducing further systematic errors, we chose not to separate neutrino from antineutrino events. Thus both incident neutrino types were included in the Monte Carlo simulation with the appropriate proportion. The data were analyzed in several stages to emphasize particular aspects of the standard model of opposite-sign dimuon production. In particular, the x_{vis} distribution was analyzed for the CKM terms and the magnitude of the strange sea, given by κ. The ratio of the number of dimuon events normalized to the number of single-muon events plotted as a function of visible energy was used to check the slow rescaling feature of charm-quark production.

A. Systematic errors

The experimental systematic errors were dominated by the decay background subtraction. Our estimate of this

background was based on the assumption that essentially all of the like-sign events in our detector originated from meson decay in the hadronic shower. Thus the error of the correction was determined by the statistics of the like-sign dimuon events. This resulted in the average relative error for each bin of the background x_{vis} distribution to be $\pm 33\%$. To determine the effect of this uncertainty we repeated our analysis with the background systematically changed by $\pm 33\%$. The error arising from the uncertainty of the incident neutrino flux was also considered and found to be less than one-third of that associated with the background subtraction.

The main theoretical systematic error arose from the uncertainty of the charm-quark mass m_c. The sensitivity to m_c was estimated by allowing it to vary from 1 to 2 GeV/c^2 in the fits of the x_{vis} distribution. Another important source of systematic error arose from the uncertainty in the $(\bar{U} + \bar{D})/(U + D)$ ratio of the parametrization[16] of the quark structure functions. This uncertainty was accommodated by allowing $(\bar{U} + \bar{D})/(U + D)$ to vary by $\pm 10\%$.[21] Other sources of error, such as that due to the quoted experimental error[20] of the parameter, $\epsilon = 0.19 \pm 0.03$, in the Peterson fragmentation function, were considered and found to be small compared to the m_c and $(\bar{U} + \bar{D})/(U + D)$ uncertainties.

B. Determination of $B_c |U_{cd}|^2$ and $B_c \kappa |U_{cs}|^2$

The first stage of the analysis was to determine the cross-section factors $B_c |U_{cd}|^2$ and $B_c \kappa |U_{cs}|^2$ by fitting[22] a Monte Carlo–generated x_{vis} distribution to the data, assuming that the charm quark mass $m_c = 1.5$ GeV/c^2. The fitting procedure was sensitive to both the magnitude and the shape of the x_{vis} distribution. In our modeling of the theory, we assumed that both the nonstrange quark sea and valence distributions had the same shapes and magnitudes as given in Ref. 16. The magnitude of the strange sea was allowed to vary, but its shape was given
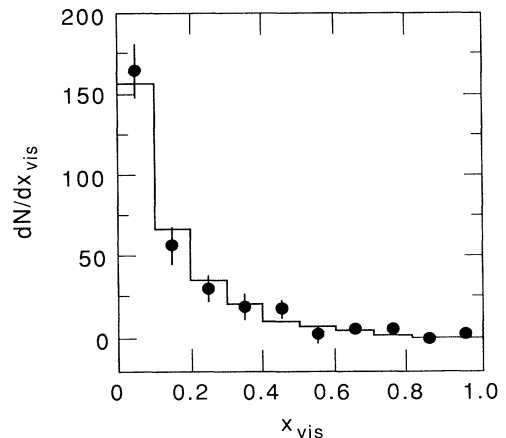
FIG. 4. The x_{vis} distribution for background-subtracted dimuon events (points with errors) and the best-fit Monte Carlo simulation (unbroken line) described in the text. Note that neutrino and antineutrino events were not separated.

TABLE III. The results of the fits to the x_{vis} distribution. The central values of the fit parameters were computed with $m_c = 1.5$ GeV/c^2. The indicated systematic errors associated with the branching ratio B_c, the background subtraction, the charm-quark mass m_c, and the $\overline{Q}/Q$ ratio have been added in quadrature.

Parameter	Value	Statistical error	Systematic error
Fit 1:			
$\chi^2/N_{\mathrm{DF}} = 1.23$			
$B_c\|U_{cd}\|^2$	(4.27	±1.44	$^{+0.96}_{-0.73}) \times 10^{-3}$
$B_c\kappa\|U_{cs}\|^2$	(4.42	±0.86	$^{+0.93}_{-0.46}) \times 10^{-2}$
κ (from ratio)	0.533	±0.215	$^{+0.044}_{-0.0062}$
Fit 2: Wolfenstein parametrization of CKM matrix (Ref. 23). $B_c = 11.3 \pm 1.5\%$			
$\chi^2/N_{\mathrm{DF}} = 1.23$			
$\lambda = \|U_{cd}\|$	0.194	±0.033	$^{+0.025}_{-0.021}$
κ	0.407	±0.075	$^{+0.103}_{-0.069}$

by the parametrization of Ref. 16. The result was that

$$B_c|U_{cd}|^2 = (4.27 \pm 1.44 \pm 0.71^{+0.64}_{-0.14} \pm 0.097) \times 10^{-3} ,$$

and

$$B_c\kappa|U_{cs}|^2 = (4.42 \pm 0.86 \pm 0.22^{+0.81}_{-0.05} \pm 0.40) \times 10^{-2} ,$$

where the first error was from statistical sources, the second from the background subtraction error, the third from allowing the charm mass to vary by ± 0.5 GeV/c^2 about 1.5 GeV/c^2, and the fourth from the $\pm 10\%$ uncertainty in the ratio $(\overline{U} + \overline{D})/(U + D)$. (Note that hereafter we quote only the total systematic error computed by adding all sources in quadrature.) Figure 4 shows that the data agree with Monte Carlo for these fit values. The details of the results are summarized in Table III.

C. Determination of $|U_{cd}|^2$, $\kappa|U_{cs}|^2$, and κ

The terms $|U_{cd}|^2$ and $\kappa|U_{cs}|^2$ themselves may be computed from the results of the fit described above by fixing the value of the charmed-meson branching ratio at the best known value of $B_c = (11.3 \pm 1.5)\%$.[23] The result was

$$|U_{cd}|^2 = 0.0378 \pm 0.0127^{+0.0099}_{-0.0082} ,$$

and

$$\kappa|U_{cs}|^2 = 0.391 \pm 0.076^{+0.097}_{-0.066} ,$$

where the first errors were from the statistical significance of our data and the second from combined systematic errors from the sources enumerated above, including the quoted error of B_c.

If we evaluate the ratio of $\kappa|U_{cs}|^2$ to $|U_{cd}|^2$ and take the CKM terms as given by other measurements,[24] we can obtain the strength of the strange sea independently of our assumption of the branching fraction B_c. The result was

$$\kappa = 0.533 \pm 0.215^{+0.044}_{-0.0062} ,$$

where the first error was from statistical sources and the second from systematic effects. Both the statistical and

systematic correlations were included in the computation of the errors.

D. Determination of $|U_{cs}|$ and κ

To determine $|U_{cs}|$ and κ we had to impose additional conditions in the model either by constraining $|U_{cs}|$ by the unitary bound, or by assuming that U_{cd} and U_{cs} were related through a parametrization of the CKM matrix. In the unitarity bound calculation we fixed[24] $|U_{us}| = 0.2205 \pm 0.0018$ to establish that $|U_{cs}|^2 < 0.9524$ and $\kappa > 0.274$, where both $|U_{cs}|^2$ and κ are quoted at 90% confidence limits. Alternatively, we can take the value of $\kappa|U_{cs}|^2$ determined above and assume that $\kappa < 1$ to find that $|U_{cs}| > 0.511$ at the 90% confidence limit. Statistical and systematic errors were combined in quadrature to compute these limits.

The fraction of the strange sea κ can be separated from the CKM term $|U_{cs}|$ by using the parametrization of the CKM matrix given in Ref. 25. In this parametrization $U_{cd} = \lambda$ and $U_{cs} = 1 - \lambda^2/2$, where λ is approximately equal to the sine of the Cabibbo angle. We performed a fit, setting $m_c = 1.5$ GeV/c^2, to determine

$$\lambda = 0.194 \pm 0.033(\text{stat})^{+0.025}_{-0.021}(\text{syst}) ,$$

and

$$\kappa = 0.407 \pm 0.075(\text{stat})^{+0.103}_{-0.069}(\text{syst}) .$$

Figure 5 summarizes the various theoretical contributions to the experimental x_{vis} distribution. Note that the neutrino term dominates the antineutrino contribution in our data. Shown are the nonstrange valence and sea and the strange sea contributions to the experimental x_{vis} distribution. The latter two contributions are for ν and $\overline{\nu}$ data combined.

E. Kinematic properties of dimuon events

As a check of the model of opposite-sign dimuon production we studied the threshold dependence of the production cross section. Figure 6 shows the ratio of the
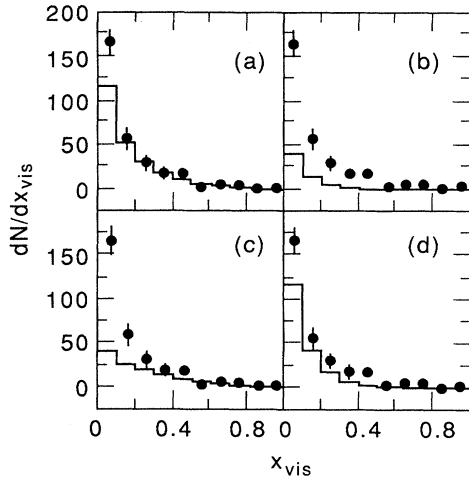
FIG. 5. The various theoretical parts (solid lines) of the measured x_{vis} distribution (data points with error flags) showing (a) neutrino, (b) antineutrino contributions, (c) nonstrange-, and (d) strange-quark contributions for ν and $\bar{\nu}$ data combined. Note that the data distribution is repeated in each part of the figure. The subfigures indicate that the neutrino dominates the antineutrino contribution, and the strange quark (ν and $\bar{\nu}$ combined) dominates the nonstrange contribution.

number of dimuon events (neutrino and antineutrino events together) to neutrino charged-current events as a function of the visible energy, defined by $E_{vis} = \nu_{vis} + E_{\mu 1}$. In dimuon events the undetected outgoing neutrino from the semileptonic decay of the charmed particle carries on average 10% of the total event energy, hence $E_{vis} \approx 0.9 E_{\nu}$. The data shown in the figure clearly indicate the threshold dependence, which in the standard model is controlled by the kinematic factors associated with the finite charm-quark mass included in Eq. (1).

We checked the model of dimuon production by using
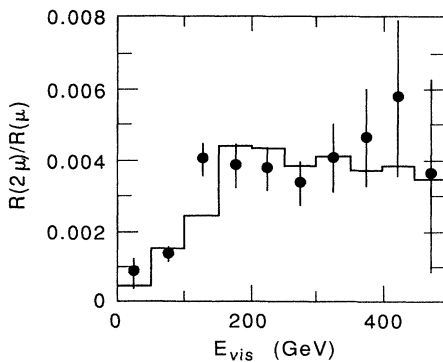
FIG. 6. The ratio of opposite-sign dimuon production to neutrino-nucleon charged-current scattering as a function of visible energy, $E_{vis} = E_{shower} + E_{\mu 1} + E_{\mu 2}$. The data points are indicated by the error flags and the fit by the solid line. In the fit the CKM terms and κ are fixed to the value given in Table III and only the charm-quark mass was allowed to vary.
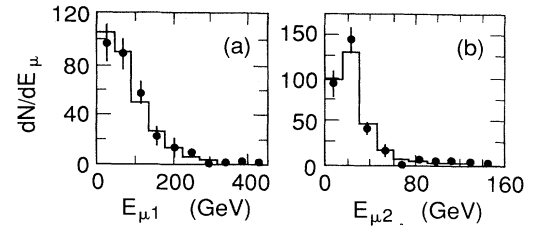
FIG. 7. Comparison of muon energies, (a) leading, and (b) nonleading, with the Monte Carlo simulation. The data are indicated by the points with the error flags, and the Monte Carlo simulation by the solid line.

the excitation curve to determine the effective mass of the charm quark m_c taking the branching ratio B_c, κ, and the CKM matrix terms to be fixed at the values determined by our fits. (See Table III.) Note that this is only a consistency check of the analysis and not a fit for the charm-quark mass since we have determined the value of κ and the CKM terms assuming $m_c = 1.5$ GeV/c^2. The result of the check was

$$m_c = [1.91 \pm 0.28(\text{stat})^{+0.45}_{-0.55}(\text{syst})] \text{ GeV}/c^2$$

($\chi^2 = 17.6$ for 9 degrees of freedom for statistical errors only).[26] We note that this result is within the range of the charm-quark mass, $m_c = 1.5 \pm 0.5$ GeV/c^2, assumed in our fits. Here we quote only the systematic error from the background subtraction, which was our chief experimental uncertainty.

The fine-grained structure of our neutrino detector allowed good measurements of the kinematic properties of opposite-sign dimuons. In Fig. 7 we show the energy distributions of the leading and trailing muons. Superimposed are the simulated distributions with $m_c = 1.5$ GeV/c^2. The P_t distributions of the leading and trailing muons are compared with Monte Carlo data in Fig. 8. The good agreement in this figure confirmed the validity of the kinematics simulation of the dimuon production as well as the transverse-momentum parametrization used. Another interesting check is the distribution in the experimental fragmentation quantity defined as
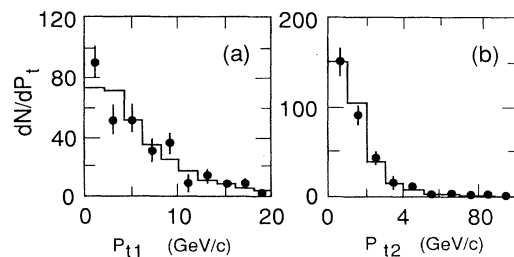
FIG. 8. The transverse-momentum distributions of (a) leading, and (b) nonleading muons with respect to the hadronic shower direction determined from energy-flow measurements are compared with the Monte Carlo simulation (solid line).
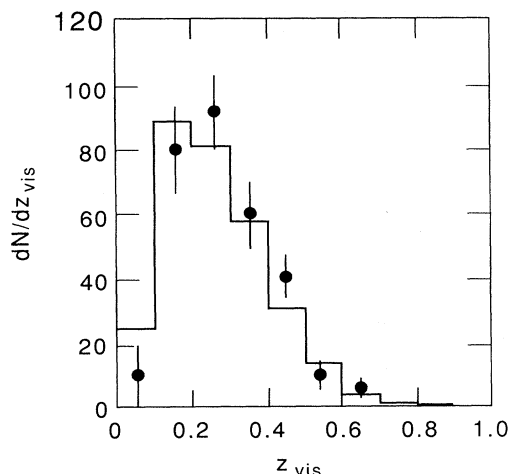
FIG. 9. The experimental fragmentation distribution compared with Monte Carlo simulation (solid line).

FIG. 10. The angle between the muons in a plane perpendicular to the incident neutrino direction required compared with the dimuon production model (solid line).

$Z_{\text{vis}} = E_{\mu 2}/(E_{\mu 2} + E_{\text{shower}})$ shown in Fig. 9. Again the Monte Carlo simulation agrees well with the data. Finally, in Fig. 10 we demonstrate that the angle between the two muons in a plane perpendicular to the incident neutrino direction is consistent with our simulation of the process.

V. SUMMARY

We have performed fits of both the magnitude and shape of the x_{vis} distribution of opposite-sign dimuon events to the prediction based on the standard model. We found that

$$B_c |U_{cd}|^2 = [4.27 \pm 1.44(\text{stat})^{+0.96}_{-0.73}(\text{syst})] \times 10^{-3} ,$$

$$\kappa B_c |U_{cs}|^2 = [4.42 \pm 0.86(\text{stat})^{+0.93}_{-0.46}(\text{syst})] \times 10^{-2} .$$

Assuming a semileptonic branching ratio $B_c = (11.3 \pm 1.5)\%$, we have determined

$$|U_{cd}|^2 = 0.0378 \pm 0.0127(\text{stat})^{+0.0099}_{-0.0082}(\text{syst}) ,$$

and

$$\kappa |U_{cs}|^2 = 0.391 \pm 0.076(\text{stat})^{+0.097}_{-0.066}(\text{syst}) .$$

Taking the ratio of these terms and using the CKM elements given by Ref. 24, we found

$$\kappa = 0.533 \pm 0.215(\text{stat})^{+0.044}_{-0.0062}(\text{syst}) .$$

Assuming the form of the CKM matrix given by Ref. 25, we determined the ratio of strange to nonstrange sea quarks in the nucleon was

$$\kappa = 0.407 \pm 0.075(\text{stat})^{+0.103}_{-0.069}(\text{syst}) .$$

The data are consistent with the hypothesis that opposite-sign dimuons in neutrino-nucleon scattering arise from charm-quark production, which fragments into a charmed meson, followed by its semileptonic decay. Our results agree with other measurements at these energies,[27,28] and with data taken at lower energy.[29,30] No evidence of a new source of opposite-sign dimuons with a high-energy threshold has been observed. Analysis of additional data taken at a subsequent time is in progress.[31]

ACKNOWLEDGMENTS

*Present address: Varian Associates, Palo Alto, CA 94303.

†Present address: Fermilab, Batavia, IL 60510.

‡Present address: Argonne National Laboratory, Argonne, IL 60439.

§Present address: AT&T Bell Telephone Laboratories, Naperville, IL 60566.

**Present address: Deutsches Elektronen-Synchrotron, Hamburg, Germany

††Present address: Physics Dept., University College London, London WC1E 6BT, England.

‡‡Present address: Dept. of Physics, Florida State Univ., Tallahassee, FL 32306.

[1]This analysis was taken largely from B. Strongin, Ph.D. thesis, MIT, 1989.

[2]J. Kaplan and F. Martin, Nucl. Phys. B115, 333 (1976); C. H. Lai, Phys. Rev. D 18, 1422 (1978); B. J. Edwards and T. D. Gottschalk, Nucl. Phys. B186, 309 (1981).

[3]N. Cabibbo, Phys. Rev. Lett. 10, 531 (1963); M. Kobayashi and T. Maskawa, Prog. Theor. Phys. 49, 652 (1973).

[4]R. M. Barnett, Phys. Rev. D 14, 70 (1976); J. Kaplan and F. Martin, Nucl. Phys. B115, 333 (1976); R. Brock, Phys. Rev. Lett. 44, 1027 (1980); H. Georgi and H. D. Politzer, Phys. Rev. D 14, 1829 (1976).

[5]U. Amaldi et al., Phys. Rev. D 36, 1385 (1987).

[6]Neutrino-emulsion data: N. Ushida *et al.*, Phys. Lett. **121B**, 287 (1983); **121B**, 292 (1983); Phys. Lett. B **206**, 375 (1988); **206**, 380 (1988). CKM terms and semileptonic branching ratios: F. J. Gilman, K. Kleinknecht, and B. Renk, Report No. SLAC-Pub-5155, 1989 (unpublished).

[7]D. Hitlin, in *Lepton and Photon Interactions,* proceedings of the International Symposium on Lepton and Photon Interactions at High Energies, Hamburg, West Germany, 1987, edited by W. Bartel and R. Ruckl [Nucl. Phys. B (Proc. Suppl.) **3**, 179 (1987)].

[8]D. Bogert *et al.*, IEEE Trans. Nucl. Sci. **NS-29**, 363 (1982); T. S. Mattison, *et al.*, Phys. Rev. D **42**, 1311 (1990).

[9]S. Fuess *et al.*, in *Proceedings of the Gas Sampling Calorimeter Workshop,* Batavia, Illinois, 1982, edited by M. Atac (Fermilab, Batavia, 1982), p. 241; M. Tartaglia *et al.*, in *Proceedings of the Gas Sampling Workshop,* Batavia, Illinois, 1985, edited by M. Atac, G. Brandenburg, and M. Mishina (Fermilab, Batavia, 1986), p. 259.

[10]A. Mukherjee, Ph.D. thesis, MIT, 1986.

[11]T. Sjostrand, Comput. Phys. Commun. **27**, 243 (1982).

[12]U. Schneekloth and M. Tartaglia, E733 Memo 88-4, Fermilab, Box 500, Batavia, IL 60510.

[13]B. Schumm *et al.*, Phys. Rev. Lett. **60**, 1618 (1988); H. Burkhardt *et al.*, Z. Phys. C **31**, 39 (1986).

[14]B. Strongin (Ref. 1).

[15]L. Stutte, N Center Wide Band Neutrino Beam, Fermilab Tech. Memo TM-1305, Box 500, Batavia, IL 60510.

[16]The cross sections used in this analysis were developed from the set-1 parametrization of the quark structure functions of D. W. Duke and J. F. Owens, Phys. Rev. D **30**, 49 (1984). The same quark structure function parametrization was employed to simulate opposite-sign dimuon production.

[17]R. Blair *et al.*, Phys. Rev. Lett. **51**, 343 (1983); P. Berge *et al.*, Z. Phys. C **35**, 443 (1987).

[18]V. Barger and R. J. N. Phillips, Phys. Rev. D **14**, 80 (1976).

[19]M. Aguilar-Benitez *et al.*, Phys. Lett. **123B**, 103 (1983).

[20]C. Peterson *et al.*, Phys. Rev. D **27**, 105 (1983). The value of ϵ was fixed to the value determined by the ARGUS Collaboration, H. Albrecht *et al.*, Phys. Lett. **150B**, 235 (1985).

[21]We have compared the predicted $\bar{Q}/Q$ ratio of the Duke and Owens parametrization (Ref. 16) using our value of κ to that of several other parametrizations [E. Eichten, I. Hinchliffe, K. Lane, and C. Quigg (EHLQ), Rev. Mod. Phys. **56**, 579 (1984); **58**, 1047 (1986); M. Diemoz *et al.*, Z. Phys. C **39**, 21 (1988); J. V. Allaby *et al.*, Phys. Lett. B **197**, 281 (1987)] at their respective Q_0^2 normalization points. We found agreement within 3% in all cases, with the exception of EHLQ set 1, where the agreement was within 18%. We have also compared our value of $\bar{Q}/Q=0.183$ (simulated by the Ref. 16 parametrization) with the CERN-Dortmund-Heidelberg-Saclay (CDHS) $\bar{Q}/Q=0.158\pm0.025$ value determined from data taken at lower energies [H. Abramowicz *et al.*, Z. Phys. C **15**, 19 (1983)]; and with the Columbia-Chicago-Fermilab-Rochester (CCFR) value taken in the same beam as our experiment (M. H. Shaevitz, NEVIS-R-1482), where $\bar{Q}/Q=0.175\pm0.012$.

[22]F. James and M. Roos, CERN Compute Library Writeup No. D506 Minuit (1981.12.01/1989.09.12).

[23]We used the value of B_c computed in F. J. Gilman *et al.*, Report No. SLAC-Pub-5155, 1989 (unpublished), based on the data of Refs. 6 and 7.

[24]Particle Data Group, J. J. Hernández *et al.*, Phys. Lett. B **239**, 1 (1990).

[25]L. Wolfenstein, Phys. Rev. Lett. **51**, 1945 (1983). We used this parametrization of the CKM matrix up to order λ^2. The higher-order terms associated with *CP* violation were considered to be small.

[26]We do not have sufficient statistics to iterate our solution, or to simultaneously fit for m_c and the other parameters of the theory.

[27]CCFR Tevatron data: C. Foudas *et al.*, Phys. Rev. Lett. **64**, 1207 (1990).

[28]V. Jain *et al.*, Phys. Rev. D **41**, 2057 (1990).

[29]CCFR Collaboration: K. Lang *et al.*, Z. Phys. C **33**, 483 (1987).

[30]CDHS Collaboration: H. Abramowicz *et al.*, Z. Phys. C **15**, 19 (1982).

[31]R. Hatcher (in preparation), Michigan State University, E. Lansing, MI 48824.